Polymer Chemistry

Influence of block sequence on the colloidal self-assembly of poly(norbornene)-block-poly(ethylene oxide) amphiphilic block polymers using rapid injection processing

Journal:	*Polymer Chemistry*
Manuscript ID	PY-ART-06-2019-000954.R1
Article Type:	Paper
Date Submitted by the Author:	08-Aug-2019
Complete List of Authors:	Lang, Chao; Pennsylvania State University, Materials Science and Engineering Kumar, Manish; Pennsylvania State University, Chemical Engineering Hickey, Robert ; Pennsylvania State University, Materials Science and Engineering; Pennsylvania State University

Influence of block sequence on the colloidal self-assembly of poly(norbornene)-block-poly(ethylene oxide) amphiphilic block polymers using rapid injection processing

Chao Lang,[a,b] Manish Kumar,[b,c,d,e] Robert J. Hickey[a,c,*]

[a]*Department of Materials Science & Engineering,* [b]*Department of Chemical Engineering,* [c]*Materials Research Institute,* [d]*Department of Biomedical Engineering,* [e]*Department of Civil and Environmental Engineering, The Pennsylvania State University, University Park, PA, 16802 USA*

Abstract

An accessible and robust method for preparing colloidal nanostructures from amphiphilic block copolymers is of significant interest due to their wide-spread usage in biomedical applications. Traditional colloidal block copolymer self-assembly methods such as slow water addition, film rehydration, and electroformation are often costly and time-consuming due to the lengthy preparation procedures. Rapid injection, where the initial amphiphilic block copolymer is dissolved in a good solvent, and rapidly injected into a selective solvent, offers a convenient, effective, and versatile approach for preparing colloidal nanostructures. A better understanding of the self-assembly mechanism and guiding principles will allow broad implementation of rapid injection mediated block copolymer self-assembly for a variety of applications. Another important prerequisite and driving force in nanostructured polymer materials is to develop innovative polymerization methods capable of generating block copolymers with different polymer chemistries as well as molecular architectures. In the work presented here, poly(norbornene)-*block*-poly(ethylene oxide) (NO) diblock and NON triblock copolymers were synthesized by using two controlled polymerization methods: ring opening metathesis polymerization (ROMP) and living anionic polymerization (LAP). The self-assembly behaviors of AB diblock and ABA triblock copolymers were studied using rapid injection. A variety of colloidal nanostructures including spherical micelles, worm-like micelles, vesicles, and microgels were readily prepared by tuning polymer concentration and architecture. Due to

the robustness of the self-assembly process, hydrophobic gold nanoparticles (AuNP) can be co-assembled with the block copolymers as an accessible strategy to install functionality into nanostructures. Combining innovative polymerization and processing methods, various colloidal structures with desired functionality can be readily prepared in a controlled manner. The findings presented here are beneficial for developing a selection of block copolymer-based colloidal systems with applications in various technologically important areas, such as drug delivery, nanomedicine, and diagnostics.

Introduction

Block polymers formed by covalently connecting incompatible polymer chains can self-assemble into numerous nanostructures in bulk and in solution.[1-3] These self-assembled nanostructures have found tremendous applications in various areas, such as thermoplastic elastomers,[4] organic electronics,[5,6] drug delivery,[7-9] diagnostics,[10] tissue engineering,[11,12] artificial enzymes[13,14] and separation membranes.[15-17] The resulting equilibrium state of block copolymer self-assembly is a balance between maximization of chain conformational degrees of freedom and reduction of the interfacial area between different polymer blocks. Over the past few decades, significant progress has been made in understanding the fundamental principles of block copolymer self-assembly in the equilibrium state.[18] However, conventional equilibrium processing methods for making aqueous colloidal polymer assemblies such as slow water addition,[19,20] film rehydration,[21] and electroformation[22] are usually time-consuming or require specialized set-ups for obtaining high-quality samples. These complexities have been a major hurdle for large-scale applications and commercialization of block copolymer self-assembly based materials. Thus, it is of significant interest to find a straightforward and robust method for preparing colloidal nanostructures from amphiphilic block copolymers. To this end, rapid injection, a method widely used for preparing supramolecular colloidal structures[23-26] has emerged as a potential alternative for polymer systems.[27] In rapid injection, molecules to be assembled are first dissolved in a good solvent and then injected into a selective solvent, which can yield large amounts of high-quality colloidal assemblies in a short time.[23-26] Establishing a similar approach for block copolymer self-assembly will enable an expeditious platform to produce polymeric colloidal nanostructures, which is also beneficial for adapting lab-scale systems to real-world manufacturing. Thus, it has been a key task to understand the mechanism, guiding principles, and tuning parameters of applying rapid injection processing for colloidal block copolymer self-assembly.

Another driving force and prerequisite in advancing block copolymer self-assembly is the development of new synthetic methods for preparing block copolymers with different polymer chemistries and architectures.[18] Controlled polymerization methods such as living anionic polymerization (LAP),[28,29] ring opening metathesis polymerization (ROMP),[30,31] atom transfer

radical polymerization (ATRP),[32,33] and reversible addition-fragmentation chain transfer (RAFT)[34] have enabled the synthesis for polymers of different compositions and molecular structures. An even more compelling and convenient strategy is to combine different controlled polymerization methods together, which can lead to block copolymers with controlled molecular weight, narrow molecular weight distribution, and efficient end-group functionality. One way to combine different polymerization methods is to end-functionalize the first polymerized block and use it to initiate the polymerization of other blocks. Some examples of polymerization methods combinations include ATRP-RAFT,[35,36] ROMP-ATRP,[37,38] ROMP-RAFT,[39] and ROMP-LAP.[40,41] Another way is to functionalize polymer blocks with different functional groups and link them together through end-to-end coupling reactions,[42] such as azide-alkyne cycloaddition,[43,44] thiol-ene addition,[45,46] thiol-maleimide addition[47] and termination-mediated coupling reaction.[48] Compared to other coupling techniques, termination-mediated coupling reactions require fewer synthetic steps (only need to functionalize one polymer block) and have high coupling efficiencies, making them preferable for synthesizing well-defined block copolymers.[31,48]

The molecular architecture or topology of amphiphilic block copolymers has a profound effect on the self-assembled structures of colloidal aggregates.[49-54] Typical linear AB amphiphilic block copolymers have been shown to self-assemble into spherical micelles, worm-like micelles, vesicles, bilayers, and large complex micelles or vesicles, which are dependent on not only the volume fraction of the hydrophilic polymer block, but on polymer concentration and solvent quality.[50] By adding a third polymer block, for example to create an ABA-type polymer in which the A-block is hydrophobic, the resulting self-assembled structures in water change significantly. At low concentrations, spherical micelles with a "flower-like" morphology form, where the two hydrophobic A-blocks will reside in the same spherical domain, and the mid B-block will create a loop.[55] With increasing ABA polymer concentration, physically-crosslinked gels form at a critical gelation concentration (CGC), and the hydrophobic A-blocks reside in different domains with the mid B-block bridging the domains.[56-58] If the polymer composition and architecture change to an ABC-type, where one block is hydrophilic and all three blocks are immiscible, complex multicomponent colloidal

aggregates form. In addition to increasing the polymer complexity, the ABC-type polymer architecture can be either linear or miktoarm star,[59] which expands the morphological phase space that includes segmented or compartmentalized colloidal aggregates.[60] Additional non-linear amphiphilic polymers with diverse self-assembled morphologies encompass grafted, bottlebrush, dendritic, and cyclic polymers.[51-54,61] Fully establishing the phase behavior of colloidal aggregates using diverse chemical compositions and chain architectures is only just underway. In addition to fundamentally understanding the thermodynamic driving forces leading to self-assembled morphologies, systematic studies are needed to identify the effects of different processing methods on colloidal self-assembly of amphiphilic block copolymers.[62]

Here, a combination of LAP and ROMP are used to synthesize AB and ABA-type amphiphilic block copolymers, and to explore the self-assembly behavior using rapid injection processing. PEO, synthesized using LAP, with a hydroxyl end-group was functionalized with a terminal benzaldehyde, was used to terminate a Schrock carbene catalyzed ROMP polymerization of poly(norbornene) (PNBE, N), affording the diblock copolymer. By using commercially available PEO with two hydroxyl end-groups, ABA triblock copolymers with two hydrophobic ends were successfully synthesized, suggesting the strategy may be further applied for synthesis of more complex polymers such as multiblock copolymers, grafted branch copolymers, and biomass-based hybrid copolymers.[63,64] The self-assembly of the newly synthesized AB diblock and ABA triblock copolymers was studied using rapid injection processing in which the polymers are initially dissolved in a good solvent (tetrahydrofuran, THF) and then injected into a B-selective solvent (water). We find that the AB diblock copolymers self-assemble into spherical micelle, worm-like micelle, and vesicles as the initial polymer concentration is increased. On the other hand, the ABA triblock copolymers self-assemble into spherical micelles that are either “flower-like” or physically-crosslinked spherical micellar aggregates over the same concentration range as the AB diblock copolymer (**Figure 1**). To further add functionality to the system, gold nanoparticles (AuNPs) were co-assembled with NON to afford nanocomposite microgels exhibiting plasmonic properties. The work presented here using rapid injection processing for preparing block copolymer-based nanomaterials has the potential to be further translated to techniques that are suitable for large-

scale applications.

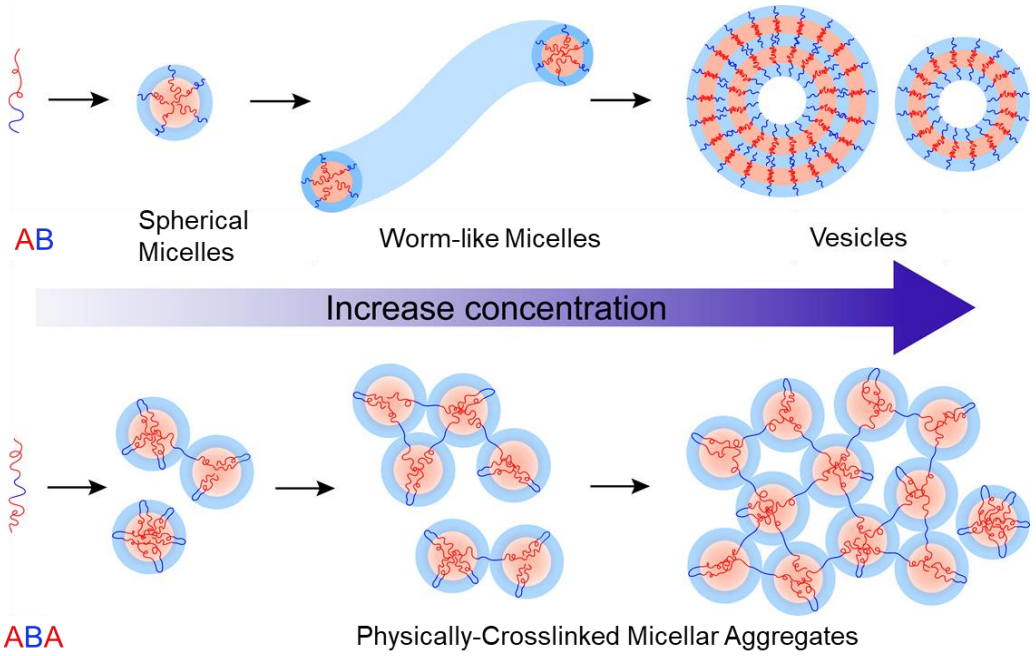

Figure 1. A schematic illustration of different self-assembly routes for AB diblock and ABA triblock copolymers (the A- and the B-blocks are hydrophobic and hydrophilic, respectively) at different concentrations when using a rapid injection processing method.

Experimental

Methods

Organic solvents used for synthesis were used directly from a solvent drying system (JC Meyer Solvent Systems). Nuclear magnetic resonance (NMR) experiments were performed on an Avance AV3HD 500 NMR spectrometer (Bruker) at room temperature. All of the obtained spectra were calibrated according to the residual solvent peak. The size-exclusion chromatography (SEC) experiments were performed on an EcoSEC HLC-8320GPC (Tosoh Bioscience) with tetrahydrofuran (THF) as the mobile phase. The instrument was equipped with a Wyatt DAWN Heleos-II eight-angle static light scattering (SLS) detector (Wyatt Technology). Cryogenic transmission electron microscopy (cryo-TEM) samples were prepared using a FEI Vitrobot, and stored and handled in the frozen state in liquid nitrogen. The samples were imaged in low-dose mode.

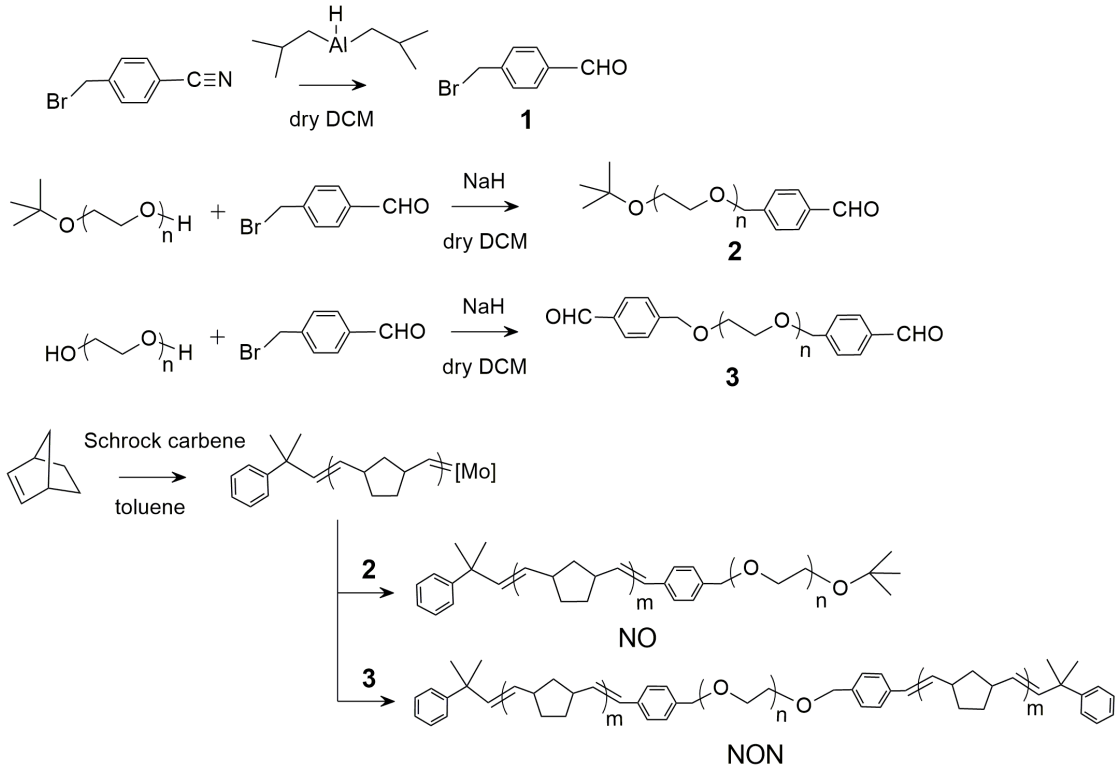

Scheme 1. Synthetic routes for NO diblock and NON triblock copolymers.

Synthesis of 4-(bromomethyl)benzaldehyde 1

Compound **1** (**Scheme 1**) was synthesized according to a previously reported method with modification.[65] 6.6 g (33.7 mmol) of α-bromo-p-tolunitrile was dissolved in 80 mL of anhydrous methylene chloride (DCM), and purged with argon. The solution was then cooled down with an ice bath before 44 mL of 1.0 M diisobutylaluminum hydride (Caution: Extremely reactive in atmosphere, use necessary precautions) methylene chloride solution (Sigma-Aldrich) was added to the reaction using a cannula. The reaction was allowed to react at 45 °C for 3 h. After cooling the reaction down to room temperature, 200 mL of 4 wt% HCl solution was slowly added to the reaction and stirred for about 1 h. The organic phase was separated and washed with water followed by adding anhydrous Mg_2SO_4 to dry the methylene chloride solution. After evaporating the solvent under reduced pressure, the obtained yellow/white solid mixture was subjected to sublimation at 60 °C for 5 h to afford pure product as white solid (yield: 50%). ^{1}H NMR ($CDCl_3$): δ 10.0 (s, 1 H), 7.8 (d, 2 H), 7.55 (d, 2 H), 4.5 (s, 2 H).

Synthesis of mono-hydroxyl PEO

Mono-hydroxyl poly(ethylene oxide) was synthesized using previously published synthetic procedures.[66,67] First, ethylene oxide monomer (Sigma-Aldrich) (Caution: Ethylene oxide is a toxic gas, use necessary precautions) was purified twice with *n*-butyllithium (Sigma-Aldrich), and then initiated using potassium *tert*-butoxide (Sigma-Aldrich, 1.0 M in THF). The reaction was run in column purified THF (JC Meyer Solvent Systems) at 45 °C for 24 h, and then terminated using degassed methanol. The reaction mixture was precipitated in hexane to afford the mono-hydroxyl PEO as a white solid. ^{1}H NMR ($CDCl_3$): δ 3.78-3.76 (t, 1 H), 3.63 (s, 128 H), 1.18 (s, 9 H).

Synthesis of benzaldehyde functionalized PEO

To functionalize the PEO (**Scheme 1**), 2.0 g (10 mmol) of compound **1** and 2.0 g (1.4 mmol) of mono-hydroxyl PEO (or 2.7 g (0.7 mmol) of commercial di-hydroxyl functionalized PEO (Polymer Source, M_n = 4,000 g/mol)) were first dissolved in anhydrous THF, and then cooled down with an ice bath. 0.8 g (20 mmol) of sodium hydride (60 % dispersion in mineral oil) was added to the reaction, and allowed to react for 48 h at room temperature. The solvent was then evaporated under reduced pressure. The resulting mixture was then dissolved in methylene chloride, and washed with water three times. The methylene chloride phase was then collected, dried over anhydrous Mg_2SO_4, and concentrated under vacuum. The crude product was finally precipitate in cold diethyl ether twice and hexane once to afford the functionalized polymer as light yellow solid.

2: Yield: 85%. ^{1}H NMR ($CDCl_3$): δ 10.0 (s, 1 H), 7.86-7.84 (d, 2 H), 7.51-7.50 (d, 2 H), 4.64 (s, 1H), 3.63 (s, 128 H), 1.18 (s, 9 H).

3: Yield: 77%. ^{1}H NMR ($CDCl_3$): δ 9.99 (s, 2 H), 7.85-7.84 (d, 4 H), 7.51-7.50 (d, 4 H), 4.64 (s, 4 H), 3.63 (s, 364 H).

Synthesis of PNBE-PEO (NO) and PNBE-PEO-PNBE (NON)

A toluene solution of bicyclo[2.2.1]hepta-2,5-diene (norbornene, Sigma-Aldrich) monomer was freeze-pumped-thawed prior to the polymerization. The ROMP polymerizations were performed inside a glove box. A typical reaction procedure is as follows: 3 mL of 0.1 g/mL

(3.2 mmol) norbornene toluene solution was added dropwise to 4 mL of 0.03 g/mL (0.22 mmol) 2,6-diisopropylphenylimidoneophylidene molybdenum(VI) bis(t-butoxide) (Schrock carbene, Strem Chemical) in a toluene solution. The polymerization was reacted for 3 h, and terminated by adding 0.3 g benzaldehyde monofunctionalized PEO (0.22 mmol) in toluene. The solution was stirred for 24 h followed by precipitation in 200 mL isopropanol 3 times. The polymer was then freeze-dried using benzene to afford the final product as a light yellow solid.

NO: Yield: 65%. ^{1}H NMR ($CDCl_3$): δ 7.34-7.33 (d, 2 H), 7.30-7.28 (d, 2 H), 5.35-5.34 (m, 110 H), 5.21-5.20 (m, 54 H), 4.53 (s, 2 H), 3.64 (s, 128 H), 2.80-2.76 (m, 54 H), 2.44-2.42 (m, 114 H), 1.89-1.83 (m, 82 H), 1.81-1.74 (m, 164 H), 1.37-1.34 (m, 164 H), 1.19 (s, 9 H), 1.09-0.99 (m, 84 H).

NON: Yield: 71%. ^{1}H NMR ($CDCl_3$): δ 7.34-7.32 (d, 2 H), 7.29-7.26 (d, 2 H), 5.34-5.33 (m, 104 H), 5.21-5.20 (m, 32 H), 4.52 (s, 2 H), 3.64 (s, 364 H), 2.79-2.76 (m, 32 H), 2.44-2.42 (m, 104 H), 1.88-1.83 (m, 68 H), 1.79-1.73 (m, 136 H), 1.36-1.33 (m, 136 H), 1.08-0.99 (m, 68 H).

Synthesis of gold nanoparticles (AuNPs)

The AuNPs were synthesized according to a previously reported procedure.[68] In short, a light orange colored precursor solution was prepared by mixing 8 mL oleylamine (OAm, Sigma-Aldrich), 8 mL toluene, and 0.1 g gold(III) chloride trihydrate ($HAuCl_4 \cdot 3H_2O$, Sigma-Aldrich) together, and then purged with Argon for 10 min. 25 mg of *tert*-butylamine-borane complex (TBAB, Sigma-Aldrich) was mixed with 1 mL toluene and 1 mL OAm, and then was quickly added into the precursor solution. The color of the solution quickly turned purple, and then transitioned to red over time. After reacting for 1h, the AuNPs were collected by precipitating the reaction solution in 60 mL of acetone, and then centrifuging the solution at 8,500 rpm for 8 min. The AuNPs were washed with acetone and centrifuged one additional time, and finally dispersing in THF.

Self-assembly through rapid injection

Block copolymers were first dissolved in THF at desired concentrations (AuNPs were also added when needed). To start the self-assembly process, 50 μL of the polymer solution in THF

was injected into 1 mL of water in 20 s. The resulting solutions were further used for subsequent measurements. For AuNPs loading experiments, the polymer solution was first mixed with AuNPs THF solution before being injected into water.

Transmission electron microscopy (TEM) characterization

TEM images were collected using a FEI Tecnai G2 Spirit BioTwin instrument operated at 120 kV. TEM samples were prepared according to previously reported procedure with minor modifications.[69] Specifically, carbon coated TEM grids (FCF200-Cu, Electron Microscopy Sciences) were first subjected to glow discharge (PELCO easiGlow, Ted Pella Inc.) for 30 s to increase the wetting of polymer solution on the TEM grids. 3.5 μL of colloidal polymer solution was then added onto a TEM grid. The excess colloidal polymer solution on the grid was blotted off after 30 s using filtration paper. The grid was then washed by touching the grid surface to a water drop and blotted off with filtration paper. The grid was washed two more times by repeating this step. To negatively stain the sample, a drop of freshly prepared staining buffer solution (0.75 wt% aqueous uranyl formate) was applied to the grid surface and blotted off with filtration paper. This step was repeated two more times. Finally, the grid was air dried by leaving on the bench.

Results and discussion

A number of synthetic strategies have been established to install functional end groups on polymers through the termination step of a chain growth polymerization.[31] A variety of polymer end-functionalization reactions have been developed for ROMP according to the reactivity of transition metal complex catalyst towards different functional groups.[31] Here, we chose a molybdenum-based Schrock carbene as the catalyst and an aldehyde as the termination group. The synthetic approach was to functionalize polymers synthesized using LAP with benzyl aldehyde, which can then be further used to terminate molybdenum-mediated ROMP

reaction and afford block copolymers (**Figure 2**).

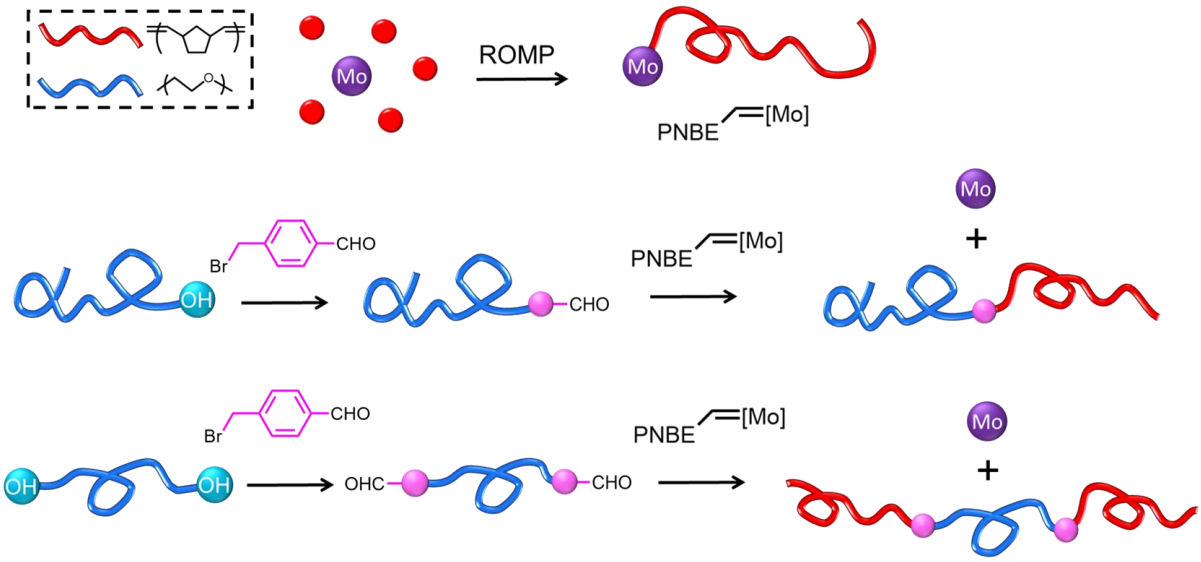

Figure 2. Schematic illustration of the synthetic strategy for block copolymers NO and NON by using a combination of LAP and ROMP.

The NO diblock copolymer was synthesized using a three-step procedure: 1) PEO with mono-functionalized hydroxy group was synthesized using LAP, 2) the hydroxyl end-group was converted to an aldehyde end-group, and 3) the aldehyde-functionalized PEO was used to terminate the polymerization of PNBE and afford diblock copolymers (**Figure 3a, Table 1**). As seen from the SEC traces, well-defined diblock copolymers were successfully synthesized by terminating ROMP with aldehyde-functionalized PEO (**Figure 3a**). Furthermore, by using commercially available PEO with two hydroxy groups, NON triblock copolymers were synthesized in a similar fashion (**Figure 3b, Table 1**). The SEC traces of the NON triblock copolymers samples show a small amount of PEO homopolymer impurities. ^{1}H NMR spectroscopy was used to characterize the polymers (**Figure 3c**). As seen from the NMR spectrum, 4-(bromomethyl)benzaldehyde molecules of high purity were synthesized. For the functionalized PEO samples, proportional number of protons from the benzaldehyde group were identified. Finally, in all block copolymer samples, peaks associated with PEO and PNBE were observed, indicating the existence of both species. By integrating the peak areas of

different blocks, PEO volume fractions were calculated (**Table 1**).

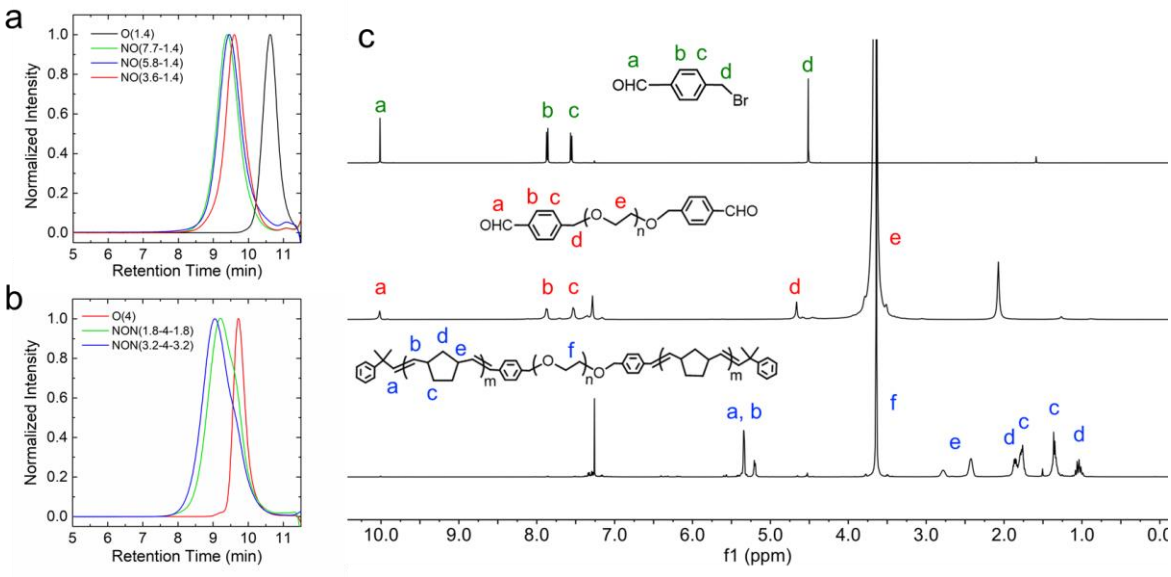

Figure 3. Characterization of the diblock and triblock copolymers synthesized by using a combination of LAP and ROMP. Size-exclusion chromatography (SEC) traces using a refractive index detector of (a) the NO diblock copolymers and (b) NON triblock copolymers of different molecular weights. (c) Stacked ^{1}H NMR spectrum of 4-(bromomethyl)benzaldehyde, difunctionalized PEO, and NON in $CDCl_3$.

Table 1. Molecular weights, dispersity values, and PEO volume fractions of diblock and triblock copolymers.

Polymer[a]	$M_{n,\,total}$[b] (kg/mol)	$Đ$[c]	f_{PEO}[d]
O(1.4)	1.4	1.48	1.00
NO(3.6-1.4)	5.0	1.21	0.25
NO(5.8-1.4)	7.2	1.37	0.17
NO(7.7-1.4)	9.1	1.49	0.13
O(4)	4.0	1.39	1.00
NON(1.8-4-1.8)	7.6	1.38	0.49
NON(3.2-4-3.2)	10.4	1.36	0.35

[a]Block copolymers are referred as AB(m-n) and ABA(m-n-m), where m and n are number-average molecular weights (kg/mol) of A and B block respectively. [b]Number-average

molecular weight of the polymers was determined from ^{1}H NMR spectroscopy. [c]Dispersity index (M_w/M_n) was determined from size exclusion chromatography (SEC). [d]PEO volume fraction (f_{PEO}) of the block copolymers was calculated using ^{1}H NMR data. We used the density of PNBE as 0.96 g mL^{-1} and PEO as 1.207 g mL^{-1} at 25 °C. The density values were used from Sigma-Aldrich.

In theory, the block copolymer synthetic procedure described here could be broadly applied to the synthesis of copolymers with different block chemistries and chain architectures. For polymers synthesized using LAP, hydroxyl groups can be precisely placed at the polymer chain-end by adding an extra ethylene oxide (EO) unit before methanol termination, which can be further converted into aldehydes and used for termination-mediated coupling reactions with ROMP.[70] Another interesting design is to use the method for converting hydroxyl groups on polysaccharides to aldehydes and synthesize biomass-based grafted or bottlebrush copolymers.[71,72] Therefore, the synthetic approach described here is versatile and enables diversity of block copolymer composition and architecture.

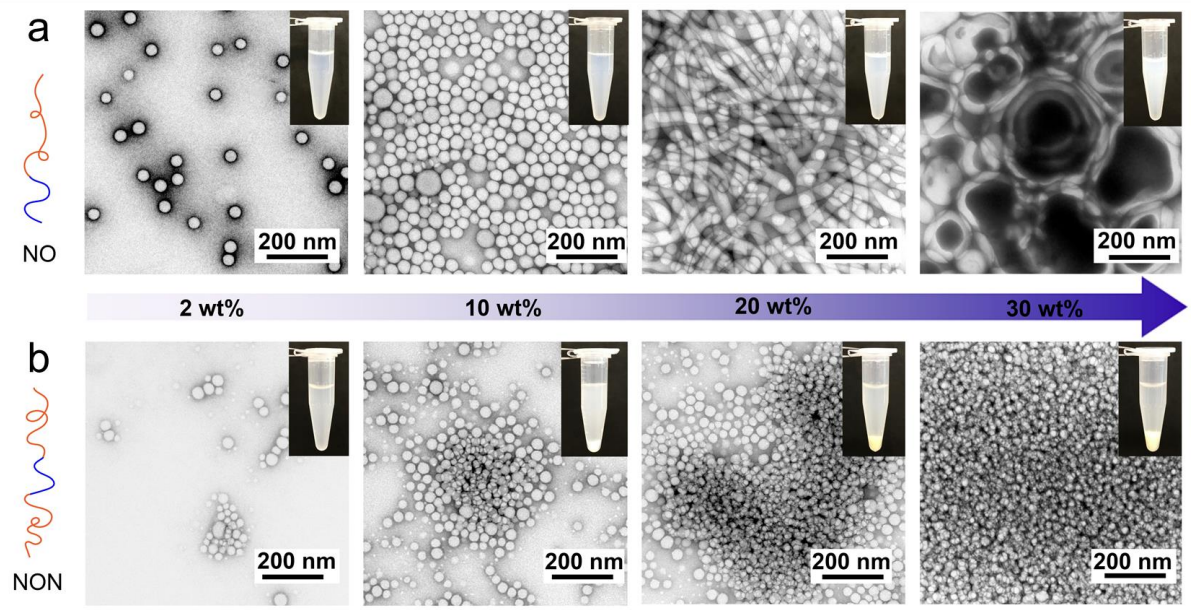

Figure 4. TEM images of NO and NON self-assembled structures in water using rapid injection processing at different polymer solution concentrations originally in THF. (a) The self-assembled colloidal structures using NO(5.8-1.4) span morphologies from spherical micelles to vesicles. (b) The self-assembled colloidal structures using NON(3.2-4-3.2) only form

spherical "flower-like" micelles and physically-crosslinked micellar aggregates. The inset images are of the aqueous polymer solutions in water after rapid injection. The samples were negatively stained with 0.75 wt% uranyl formate solution prior to imaging.

The self-assembly behaviors of representative diblock (NO(5.8-1.4)) and triblock (NON(3.2-4-3.2)) copolymers were then studied using a rapid injection processing method. The polymers were first dissolved in THF, which is a good solvent for both PNBE and PEO, at desired concentrations, and then rapidly injected into water (50 μL of polymer solution injected into 1 mL of water in 20 s). When the NO diblock copolymer is rapidly injected into water at varying initial polymer concentrations (from 2 wt% to 30 wt% in THF before injection) the solutions are colloidally stable for at least 12 hours (**Figure 4a,** inset images). In contrast, aqueous solutions formed using NON result in large polymer aggregates that settle to the bottom of the centrifuge tube when the initial polymer concentration in THF is greater than 10 wt% (**Figure 4b,** inset images). The morphologies of the self-assembled structures for the NO and NON polymers were characterized using transmission electron microscopy (TEM). All the samples for TEM were first stained with uranyl formate before imaging, which is a negative staining procedure that allows for increasing the contrast between PEO and PNBE.[69] For the NO diblock copolymer, discrete spherical micelles were observed at low initial polymer concentrations of 2 wt% and 10 wt% (**Figure 4a**). As the polymer concentration was increased to 20 wt%, worm-like micelles were formed as well as spherical micelles. At the highest initial polymer concentration (30 wt%), TEM images indicate vesicle structures were formed. The spherical micelle to worm-like micelle, and finally vesicles transition is consistent with previously reported trends for amphiphilic diblock copolymer self-assembly.[3,73] The concentration-dependent morphology transition is driven by the increase of aggregation number (N_{agg}, the average number of polymer chains in an aggregate) as polymer concentration increases. The increase in N_{agg} is favored due to the reduction in the interfacial area per chain at the hydrophobic/water interface, but results in a greater degree of polymer stretching in the hydrophobic micelle core, which is unfavorable. As N_{agg} increases, the free energy associated with polymer chain stretching becomes greater than the reduction in interfacial area per chain,

which then drives the morphological transition from spherical micelle to worm-like micelles, and finally vesicles.[3,73]

For the NON triblock copolymer samples, a drastically different self-assembly trend was observed as compared to the NO diblock copolymer samples (**Figure 4b**). In all NON samples, spherical micelles were consistently formed over a concentration range from 2 wt% to 30 wt% (**Figure 4b**). At the lowest concentrations, isolated micelles form in which the two hydrophobic N blocks reside in the same micelle core and the middle O block creates a loop (**Figure 1**).[55] As the concentration increases, the hydrophobic end blocks will begin to bridge between hydrophobic domains, creating physical crosslinks (**Figure 1**).[57] In addition to forming physical crosslinks with increasing polymer concentration, the size of the physically-crosslinked micellar aggregates, or microgels, increases. The increase in the microgel size is what drives the aggregates to settle over time as shown in the inset images of **Figure 4b**. The structure of the NON microgel was further characterized using cryogenic TEM (cryo-TEM) (**See Supporting Information**). The cryo-TEM results are consistent with the conventional TEM images in **Figure 4**, and support the claim that the physically-crosslinked micellar aggregates form during the rapid injection process.

The difference in the resulting nanostructures between the NO diblock and the NON triblock copolymers highlights the important effect of block sequence on block copolymer self-assembly. Although the two sets of block copolymers have the same chemical composition and overall molecular weights, NO and NON exhibit drastic different colloidal phase behaviors due to different block sequences. One extra factor to be considered here is the lower PEO volume fraction of NO(5.8-1.4) (f_{PEO} = 0.17) compared to NON(3.2-4-3.2) (f_{PEO} = 0.35), where vesicle morphology might be more favored over micelles for NO(5.8-1.4). To further verify the effect of polymer architecture and eliminate the factor of volume fraction, rapid injection was performed with another amphiphilic block copolymer system, poly(isoprene)-*block*-poly(ethylene oxide) (PI-PEO, IO). Diblock copolymer IO(2.5-2.7) was first synthesized using sequential LAP, and triblock copolymer IOI(2.5-5.4-2.5) was synthesized by coupling two

IO(2.5-2.7) copolymers at the OH ends. IO(2.5-2.7) and IOI(2.5-5.4-2.5) have the same PEO volume fraction (detailed characterizations were previously reported[16]). Rapid injection was then performed with these two polymers using identical conditions. IO and IOI exhibited similar self-assembled morphologies compared to NO and NON, respectively (See Supporting Information). For the IO diblock copolymer, the solution is colloidally stable, and the TEM images indicate that worm-like micelle structures form. TEM images confirm that the microgels consist of spherical micellar aggregates for the IOI sample. An additional parameter that will potentially lead to changes in the self-assembled colloidal morphology is the rate of polymer injection. The interplay between injection rate and the rate of polymer chain exchange is not currently clear, but we hypothesize that a reduction in injection rate will lead to colloidal structures that are closer to equilibrium versus faster injection rates resulting in kinetic products.

The formation of the physically-crosslinked micellar aggregates using ABA triblock copolymers is of fundamental interested, especially due to the potential implications in biomedical applications for drug delivery.[7-9] Although the microgel structures contain bridging triblock copolymers that form the physical crosslinks, it is not directly clear at first why the final morphology of the microgels is composed of spherical micelles. In the diblock copolymer case, the transition from spherical micelles to worm-like micelles and vesicles is a balance between chain stretching and interfacial area per chain.[3,50,74] Under the rapid injection processing conditions, it seems that the role of chain stretching and interfacial area per chain still dictate the self-assembled morphology for the NO diblock copolymer. As for the NON triblock copolymer, the resulting spherical micellar aggregates persist at all polymer concentrations. We posit that the factor dominating the NON morphology trend is that once the physical crosslinks are formed in the initial stages of polymer aggregation during injection of the polymer solution into water, the system becomes kinetically trapped because hydrophobic chain exchange is essentially arrested. It is well-established that ABA triblock copolymers exhibit significantly reduced chain exchange rates between micelles when the A-block forms the micelle core.[75,76] The presence of spherical micellar aggregates in the final microgel structure suggests that in the initial stages of polymer self-assembly after injection into water

spherical aggregates form, but the state is quickly trapped due to the cessation of polymer chain exchange. Therefore, the final microgel phase is a kinetically-trapped intermediate state, which would otherwise proceed to the thermodynamically favored phase if the sell-assembly process was not impeded. The claim that the initial state of the system directly after rapid injection results in spherical micellar aggregates is supported by previously published dissipative particle dynamic simulations of the self-assembly mechanism of vesicles composed of amphiphilic molecules.[77] An additional factor that must be considered in the NON triblock copolymer assembly is the role of initial polymer concentration. As N_{agg} increases with polymer concentration, it is expected that more NON chains will bridge between hydrophobic domains, which will lead to larger microgel sizes. Therefore, by tuning the polymer architecture and initial polymer concentration, one will be able to tailor microgels of desired sizes for uses in biomedical applications.

The well-defined and unique structure of the microgels have inspired us to further explore adding functionality into this new material. An important and useful type of material is colloidal polymer-nanoparticle nanocomposites with tunable physical properties dictated by the inorganic component.[19,20,78] Utilizing the robustness of block copolymer self-assembly through rapid injection, the co-assembly of AuNPs and NON was investigated for fabricating nanocomposite microgels. Following a previously reported method, AuNPs with a size of 5.4 ± 0.5 nm were synthesized (**Figure 5a**).[68] THF solutions of AuNPs and NON were then prepared, and rapidly injected into water. As seen in **Figure 5**, the AuNPs loaded microgels were successfully obtained. Furthermore, the plasmonic properties of the AuNPs is retained after injection, which is indicated by the red color of the microgels. The supernatant of the aqueous solution also exhibits a slight red color, which is caused by the AuNPs loaded into the isolated micelles and small-sized micellar aggregates that are still colloidally stable. TEM characterization performed on the nanocomposite microgels confirm that the AuNPs resided inside the PNBE micelle cores due to the hydrophobic coating (the nanoparticles are coated with oleylamine in which the amino group is attached to the gold surface) on the AuNP surface (**Figure 5b, 5c**). At concentrations of 25 wt% with respect to NON, the AuNPs were well

dispersed in the microgels with only a few AuNPs observed per micelle (**Figure 5b, 5d**). When the concentration of AuNPs was increased to 75 wt% with respect to NON, AuNPs will preferably accumulate inside one micelle core first before filling others (**Figure 5c**). The AuNPs aggregates within the micelle cores show a tendency to be non-randomly packed, although additional characterization methods are needed to confirm AuNPs packing structures in the micelle cores (**Figure 5d**). The drastically different self-assembly behaviors of 25 wt% and 75 wt% AuNP samples highlight the importance of initial concentration dependence on polymer/nanoparticle self-assembly during rapid injection processing. Presumably, AuNPs at high concentrations will first self-assemble with each other prior to co-assembling with NON during rapid injection processing. More studies are needed regarding the detailed mechanism of AuNPs co-assembly with ABA block copolymers as well as the kinetic behaviors of AuNPs loaded microgels.[79]

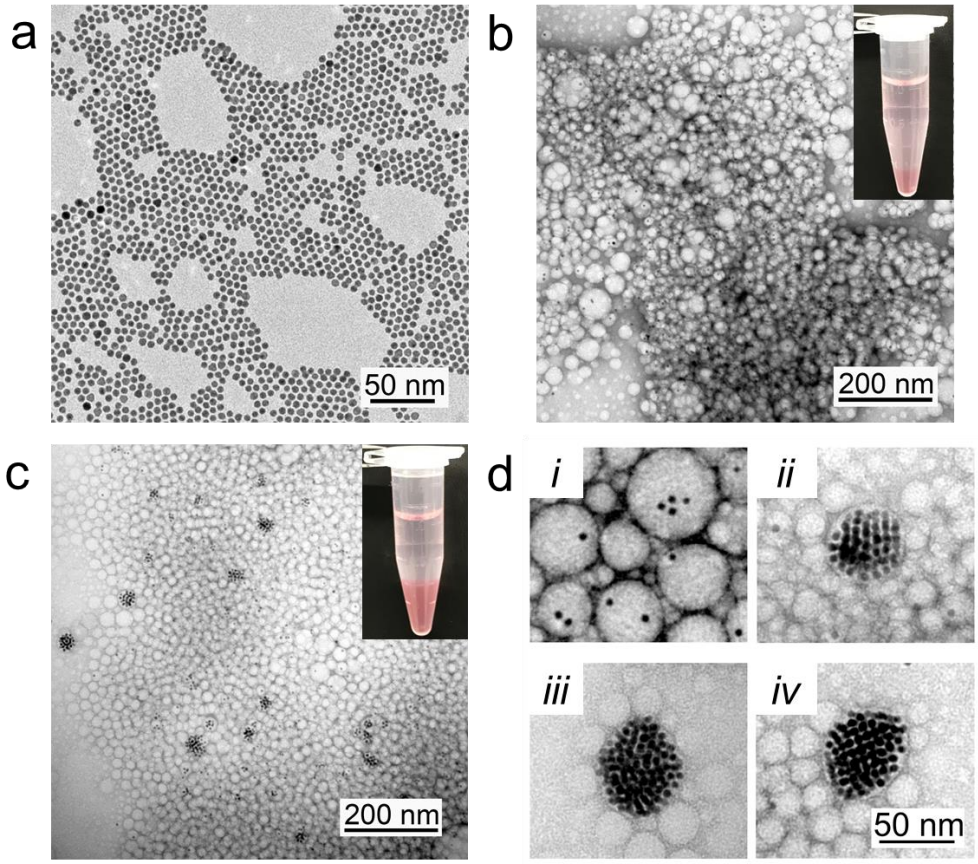

Figure 5. TEM characterization of nanocomposite microgels made with AuNPs and NON. (a) TEM image of AuNPs deposited on a TEM grid from a THF solution. The size of the AuNPs is 5.4 ± 0.5 nm. (b, c) Nanocomposite microgels from rapid injection of a THF solution of 20

wt% NON(3.2-4-3.2) with AuNPs at (b) 25 wt% and (c) 75 wt% of AuNPs with respect to polymer. Inset images show aqueous polymer solutions after rapid injection. All TEM samples were negatively stained with 0.75 wt% uranyl formate solution prior to imaging. (d) Higher magnification TEM images of the nanocomposite microgels: (*i*) 25 wt% and (*ii – iv*) 75 wt% of AuNPs with respect to polymer.

Summary

By using a combination of LAP and ROMP, a new synthetic strategy enabled the generation of amphiphilic block copolymers of different polymer chemistries and chain architectures. The self-assembly behaviors of synthesized amphiphilic AB diblock and ABA triblock copolymers were studied using rapid injection processing. While the AB diblock copolymers self-assemble into different morphologies (*e.g.*, spherical micelles, worm-like micelles, and vesicles), the ABA triblock copolymers form microgels that consist of physically-crosslinked micellar aggregates. Through co-assembly with AuNPs, nanocomposite microgels with AuNPs were prepared, which exhibited plasmonic optical properties. The work presented here shows the utility of rapid injection processing for preparing functional nanomaterials, which may find applications in a variety of fields such as biomedical, soft robotic, and artificial organs.

Acknowledgements

This work was supported using start-up funds from the Penn State University. Part of the work was also funded by National Science Foundation (NSF) grant CBET-1262 1552571 and US Army CERL W9132T-16-2-12640004-P00003.

Competing interests

The authors declare no competing interests.

Additional information

Supplemental information is available for this paper online.

REFERENCES

(1) Bates, F. S.; Fredrickson, G. *Phys. Today* **1999**, *52*, 32.

(2) Bates, F. S.; Hillmyer, M. A.; Lodge, T. P.; Bates, C. M.; Delaney, K. T.; Fredrickson, G. H. *Science* **2012**, *336*, 434.

(3) Mai, Y.; Eisenberg, A. *Chem. Soc. Rev.* **2012**, *41*, 5969.

(4) Koerner, H.; Price, G.; Pearce, N. A.; Alexander, M.; Vaia, R. A. *Nat. Mater.* **2004**, *3*, 115.

(5) Bouchet, R.; Maria, S.; Meziane, R.; Aboulaich, A.; Lienafa, L.; Bonnet, J.-P.; Phan, T. N.; Bertin, D.; Gigmes, D.; Devaux, D.; Armand, M. *Nat. Mater.* **2013**, *12*, 452.

(6) Zhang, S.; Lee, K. H.; Sun, J.; Frisbie, C. D.; Lodge, T. P. *Macromolecules* **2011**, *44*, 8981.

(7) Jeong, B.; Bae, Y. H.; Lee, D. S.; Kim, S. W. *Nature* **1997**, *388*, 860.

(8) Li, J.; Mooney, D. J. *Nat. Rev. Mater.* **2016**, *1*, 16071.

(9) Geng, Y.; Dalhaimer, P.; Cai, S.; Tsai, R.; Tewari, M.; Minko, T.; Discher, D. E. *Nat. Nanotechnol.* **2007**, *2*, 249.

(10) Ghoroghchian, P. P.; Frail, P. R.; Susumu, K.; Blessington, D.; Brannan, A. K.; Bates, F. S.; Chance, B.; Hammer, D. A.; Therien, M. J. *Proc. Natl. Acad. Sci. U. S. A.* **2005**, *102*, 2922.

(11) Li, M. H.; Keller, P.; Yang, J.; Albouy, P. A. *Adv. Mater.* **2004**, *16*, 1922.

(12) Lin, Z.; Cao, S.; Chen, X.; Wu, W.; Li, J. *Biomacromolecules* **2013**, *14*, 2206.

(13) Yin, Y.; Jiao, S.; Lang, C.; Liu, J. *Soft Matter* **2014**, *10*, 3374.

(14) Xu, H.; Cao, W.; Zhang, X. *Acc. Chem. Res.* **2013**, *46*, 1647.

(15) Shen, Y.-x.; Song, W. C.; Barden, D. R.; Ren, T.; Lang, C.; Feroz, H.; Henderson, C. B.; Saboe, P. O.; Tsai, D.; Yan, H.; Butler, P. J.; Bazan, G. C.; Phillip, W. A.; Hickey, R. J.; Cremer, P. S.; Vashisth, H.; Kumar, M. *Nat. Commun.* **2018**, *9:2294*.

(16) Lang, C.; Shen, Y.-x.; LaNasa, J. A.; Ye, D.; Song, W.; Zimudzi, T. J.; Hickner, M. A.; Gomez, E. D.; Gomez, E. W.; Kumar, M.; Hickey, R. J. *Faraday Discuss.* **2018**, *209*, 179.

(17) Nunes, S. P. *Macromolecules* **2016**, *49*, 2905.

(18) Bates, C. M.; Bates, F. S. *Macromolecules* **2017**, *50*, 3.

(19) Hickey, R. J.; Haynes, A. S.; Kikkawa, J. M.; Park, S.-J. *J. Am. Chem. Soc.* **2011**, *133*, 1517.

(20) Hickey, R. J.; Koski, J.; Meng, X.; Riggleman, R. A.; Zhang, P.; Park, S.-J. *ACS Nano* **2014**, *8*, 495.

(21) Taribagil, R. R.; Hillmyer, M. A.; Lodge, T. P. *Macromolecules* **2010**, *43*, 5396.

(22) Discher, B. M.; Won, Y.-Y.; Ege, D. S.; Lee, J. C.; Bates, F. S.; Discher, D. E.; Hammer, D. A. *Science* **1999**, *284*, 1143.

(23) Tang, Y.; Zhou, L.; Li, J.; Luo, Q.; Huang, X.; Wu, P.; Wang, Y.; Xu, J.; Shen, J.; Liu, J. *Angew. Chem., Int. Ed.* **2010**, *49*, 3920.

(24) Wang, L.; Zou, H.; Dong, Z.; Zhou, L.; Li, J.; Luo, Q.; Zhu, J.; Xu, J.; Liu, J. *Langmuir* **2014**, *30*, 4013.

(25) Cao, Y.; Hu, X.-Y.; Li, Y.; Zou, X.; Xiong, S.; Lin, C.; Shen, Y.-Z.; Wang, L. *J. Am. Chem. Soc.* **2014**, *136*, 10762.

(26) Chi, X.; Ji, X.; Xia, D.; Huang, F. *J. Am. Chem. Soc.* **2015**, *137*, 1440.

(27) Lang, C.; LaNasa, J. A.; Utomo, N.; Xu, Y.; Nelson, M. J.; Song, W.; Hickner, M. A.; Colby, R. H.; Kumar, M.; Hickey, R. J. *Nat. Commun.* **2019**, DOI: 10.1038/s41467.

(28) Hsieh, H.; Quirk, R. P. *Anionic polymerization: principles and practical applications*; CRC Press, 1996.

(29) Hadjichristidis, N.; Pitsikalis, M.; Pispas, S.; Iatrou, H. *Chem. Rev.* **2001**, *101*, 3747.

(30) Bielawski, C. W.; Grubbs, R. H. *Prog. Polym. Sci.* **2007**, *32*, 1.

(31) Hilf, S.; Kilbinger, A. F. *Nat. Chem.* **2009**, *1*, 537.

(32) Matyjaszewski, K.; Xia, J. *Chem. Rev.* **2001**, *101*, 2921.

(33) Matyjaszewski, K. *Macromolecules* **2012**, *45*, 4015.

(34) Chiefari, J.; Chong, Y.; Ercole, F.; Krstina, J.; Jeffery, J.; Le, T. P.; Mayadunne, R. T.; Meijs, G. F.; Moad, C. L.; Moad, G.; Rizzardo, E.; Thang, S. H. *Macromolecules* **1998**, *31*, 5559.

(35) Rowe, M. D.; Hammer, B. A.; Boyes, S. G. *Macromolecules* **2008**, *41*, 4147.

(36) Nicolaÿ, R.; Kwak, Y.; Matyjaszewski, K. *Macromolecules* **2008**, *41*, 4585.

(37) Coca, S.; Paik, H.-j.; Matyjaszewski, K. *Macromolecules* **1997**, *30*, 6513.

(38) Matson, J. B.; Grubbs, R. H. *Macromolecules* **2008**, *41*, 5626.

(39) Mahanthappa, M. K.; Bates, F. S.; Hillmyer, M. A. *Macromolecules* **2005**, *38*, 7890.

(40) Rizmi, A. C. M.; Khosravi, E.; Feast, W. J.; Mohsin, M. A.; Johnson, A. F. *Polymer* **1998**, *39*, 6605.

(41) Myers, S. B.; Register, R. A. *Macromolecules* **2008**, *41*, 5283.

(42) Kempe, K.; Krieg, A.; Becer, C. R.; Schubert, U. S. *Chem. Soc. Rev.* **2012**, *41*, 176.

(43) Hilf, S.; Hanik, N.; Kilbinger, A. F. M. *J. Polym. Sci., Part A: Polym. Chem.* **2008**, *46*, 2913.

(44) Dag, A.; Durmaz, H.; Kirmizi, V.; Hizal, G.; Tunca, U. *Polym. Chem.* **2010**, *1*, 621.

(45) Brummelhuis, N. t.; Diehl, C.; Schlaad, H. *Macromolecules* **2008**, *41*, 9946.

(46) Gress, A.; Völkel, A.; Schlaad, H. *Macromolecules* **2007**, *40*, 7928.

(47) Li, M.; De, P.; Gondi, S. R.; Sumerlin, B. S. *J. Polym. Sci., Part A: Polym. Chem.* **2008**, *46*, 5093.

(48) Notestein, J. M.; Lee, L.-B. W.; Register, R. A. *Macromolecules* **2002**, *35*, 1985.

(49) Rinkenauer, A. C.; Schubert, S.; Traeger, A.; Schubert, U. S. *J. Mater. Chem. B* **2015**, *3*, 7477.

(50) Zhang, L.; Eisenberg, A. *Science* **1995**, *268*, 1728.

(51) Williams, R. J.; Dove, A. P.; O'Reilly, R. K. *Polym. Chem.* **2015**, *6*, 2998.

(52) Zhou, Y.; Yan, D. *Chem. Commun.* **2009**, 1172.

(53) Khanna, K.; Varshney, S.; Kakkar, A. *Polym. Chem.* **2010**, *1*, 1171.

(54) Rosen, B. M.; Wilson, C. J.; Wilson, D. A.; Peterca, M.; Imam, M. R.; Percec, V. *Chem. Rev.* **2009**, *109*, 6275.

(55) Balsara, N.; Tirrell, M.; Lodge, T. *Macromolecules* **1991**, *24*, 1975.

(56) Raspaud, E.; Lairez, D.; Adam, M.; Carton, J.-P. *Macromolecules* **1996**, *29*, 1269.

(57) Semenov, A.; Joanny, J.-F.; Khokhlov, A. *Macromolecules* **1995**, *28*, 1066.

(58) Seitz, M. E.; Burghardt, W. R.; Faber, K.; Shull, K. R. *Macromolecules* **2007**, *40*, 1218.

(59) Hadjichristidis, N. *J. Polym. Sci., Part A: Polym. Chem.* **1999**, *37*, 857.

(60) Li, Z.; Kesselman, E.; Talmon, Y.; Hillmyer, M. A.; Lodge, T. P. *Science* **2004**, *306*, 98.

(61) Zhang, Y.; Guan, T.; Han, G.; Guo, T.; Zhang, W. *Macromolecules* **2019**, *52*, 718.

(62) Hayward, R. C.; Pochan, D. J. *Macromolecules* **2010**, *43*, 3577.

(63) Zheng, J.; Jung, S.; Schmidt, P. W.; Lodge, T. P.; Reineke, T. M. *ACS Macro Lett.* **2017**, *6*, 145.

(64) Morozova, S.; Lodge, T. P. *ACS Macro Lett.* **2017**, *6*, 1274.

(65) Fukushima, H.; Taylor, D.; Morgan, H. *Langmuir* **1995**, *11*, 3523.

(66) Masson, P.; Beinert, G.; Franta, E.; Rempp, P. *Polym. Bull.* **1982**, *7*, 17.

(67) Hadjichristidis, N.; Iatrou, H.; Pispas, S.; Pitsikalis, M. *J. Polym. Sci., Part A: Polym. Chem.* **2000**, *38*, 3211.

(68) Peng, S.; Lee, Y.; Wang, C.; Yin, H.; Dai, S.; Sun, S. *Nano Res.* **2008**, *1*, 229.

(69) Ohi, M.; Li, Y.; Cheng, Y.; Walz, T. *Biol. Proced. Online* **2004**, *6*, 23.

(70) Hillmyer, M. A.; Bates, F. S. *Macromolecules* **1996**, *29*, 6994.

(71) Vlček, P.; Janata, M.; Latalova, P.; Dybal, J.; Špírková, M.; Toman, L. *J. Polym. Sci., Part A: Polym. Chem.* **2008**, *46*, 564.

(72) Joubert, F.; Musa, O. M.; Hodgson, D. R.; Cameron, N. R. *Chem. Soc. Rev.* **2014**, *43*, 7217.

(73) Zhang, L.; Eisenberg, A. In *Macromolecular Symposia*; Wiley Online Library: 1997; Vol. 113, p 221.

(74) Zhang, L.; Eisenberg, A. *J. Am. Chem. Soc.* **1996**, *118*, 3168.

(75) Lu, J.; Bates, F. S.; Lodge, T. P. *Macromolecules* **2015**, *48*, 2667.

(76) Peters, A. J.; Lodge, T. P. *Macromolecules* **2016**, *49*, 7340.

(77) Shillcock, J. C. *Langmuir* **2012**, *28*, 541.

(78) Hickey, R. J.; Meng, X.; Zhang, P.; Park, S.-J. *ACS Nano* **2013**, *7*, 5824.

(79) Villar-Alvarez, E.; Barbosa, S.; Soltero, J. F. A.; Mosquera, V.; Taboada, P.; Rharbi, Y. *J. Phys. Chem. C* **2018**, *122*, 8553.

TOC

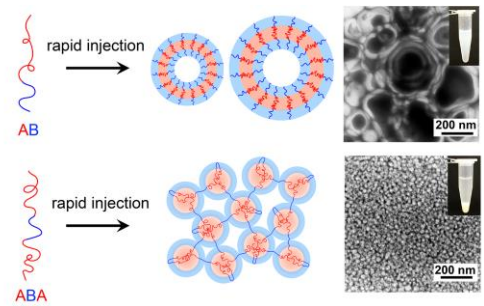

A facile self-assembly method, rapid injection, was used to study the self-assembly difference between AB diblock and ABA triblock copolymers.